GROUND BASED OPTICAL OBSERVATIONS OF SPACE DEBRIS USING CCD TECHNIQUES

T. Schildknecht, U. Hugentobler, A. Verdun, G. Beutler

Astronomical Institute, University of Berne, Switzerland

ABSTRACT

The particular charcteristics of space debris, especially their high angular velocities, require advanced observation techniques. Only CCD detectors in combination with specially designed telescopes and sophisticated tracking and image processing software will meet the specifications. The emphasis is put on the image processing techniques, special attention is paid to the difficult task of object recognition. A special section is devoted to the discussion of detection limits considering different object recognition algorithms and to the presention of simulation results. We briefly describe the experimental setup of the 50cm Laser ranging telescope in Zimmerwald and we conclude with an illustrative set of observations of objects in GEO.

1. INTRODUCTION

Optical observations using telescopes is one of the basic techniques for the detection and the tracking of objects in space. The application of the method to space debris is not common however. This is not only due to the weather dependence of optical observations but mainly due to the intrinsic faintness and potentially high angular velocities of these objects.

Let us take the geodynamic satellite LAGEOS as an example. It orbits the earth at an altitude of about 6000 km. The result is a maximum angular velocity of 240 arcsec/sec. In the Zimmerwald telescope (section 4) it crosses the field of view of 35 arcmin in 9 sec and passes over one pixel of our CCD camera in 17 msec. A satellite in a low orbit, e.g the earth observation satellite ERS-1 at an altitude of 750 km moves at up to 2000 arcsec/sec. Such an object crosses the field of view in 1 sec and one pixel of the camera is exposed to its light for merely 2 msec. For an object in an even lower orbit, the angular velocity may reach 8000 arcsec/sec.

2. SYSTEM REQUIREMENTS

The faintness and the high angular velocities of the objects lead to several rather stringent requirements for the detector and the entire system. First of all, the detector must have a high quantum efficiency. Short exposure times and a high readout-rate are required. To get accurate astrometric positions a good geometrical stability is needed and the accuracy of the epoch registration has to be in the 10 microsecond range. Furthermore a computer controlled telescope capable of tracking at high angular velocities and accelerations is necessary. Finally, the amount of real time control and processing software needed is considerable.

Charge Coupled Devices (CCD) in combination with moderate-size telescopes (apertures less than 1.5m) seem most promising to meet all of the above requirements.

3. DETECTION LIMIT

In order to detect space debris on CCD images one has to compare consecutive frames of the same sky region. Stars and other 'fixed' astronomical objects can be disregarded by subtracting images or by means of a mask generated from one of the images. Both techniques are not trivial. The first approach needs a very accurate transformation between the two frames, where both the geometry and the recorded intensities (exposure times) have to be transformed. The generation of a mask implies that every single object has to be recognized by a rather time consuming algorithm. Both methods require sidereal tracking of the telescope. Alternative techniques, e.g. to survey the geostationary ring with a fixed telescope, use the a priori knowledge concerning the movement of the stars and the satellites.

The first step of every object detection algorithm is the determination of the average background together with its variance. It may be described either with a constant value for the entire image, determined separately for several regions or modeled by a twodimensional polynomial. The main difficulty arises from the fact that the background has to be estimated from 'object free' regions whereas the objects cannot yet be recognized firmly due to the missing background. For highest accuracy requirements the background must therefore be determined iteratively. Therefore, when searching for unknown faint objects we immediately have to ask the next question of how to detect them in the noise.

The detection limit for an object crossing the field of view is given by the recorded signal-to-noise ratio. Sky background photon noise, photon noise stemming from the object itself and readout noise of the camera add up to the total noise. Using modern CCD cameras and exposure times of a few seconds, noise from the detectors dark current can be neglected.

3.1. Detection algorithms

The simplest approach to detect objects is to scan the image for pixels that have intensities above some threshold. This threshold may for instance be set at some multiple of the background rms above the background level. If a pixel exceeds this threshold, adjacent pixels can be examined and thereby all pixels belonging to the same object may be found.

To enshure with a significance level of 95% that a pixel

belongs to an object, the threshold intensity must be set to 1.7 times the rms of the background above the mean background. If any adjacent pixel is found above this level the probability for these two pixels to be part of an object is 99%. This algorithm is able to detect objects with signal to noise ratios above about 2.5 only, because the signal is always spread out over several pixels and because, although the total signal is still sufficiently strong, the individual pixels fail to reach the threshold. The signal-to-noise ratio in this case is defined as the signal integrated over all pixels of the object divided by the noise associated with the same pixels.

To observe objects with lower signal-to-noise ratios, the image can be scanned with a filter: The mean intensity of the pixels inside a 2x2 or a 3x3 box is compared with the background intensity. Maintaining a significance level of 99% for dealing with an object, one can set the threshold to only 1.2 or 0.8 times the background rms above the average background level for a 2x2 or 3x3 filter respectively which results in a minimal detectable signal-to-noise ratio of 1.2 or 0.8 respectively. In contrast to the first method we define here the signal-to-noise ratio as the ratio of the integrated values over the 2x2 or 3x3 pixel region respectively. In other words: We are not yet dealing with objects but just testing the probability that an object is present within a certain region.

Increasing the size of the filter (number of pixels) would further reduce the detection limit in terms of the above defined signal-to-noise ratio because we are correlating more and more pixels to test if they form, as an ensemble (and not as individual pixels like in the first method), an object or a part of an object. On the other hand this averaging procedure may introduce additional noise (and herewith decrease the actual signal-to-noise ratio) in the case where 'object free' pixels are added. We may therefore increase the filter size as long as it is smaller than the area covered by the object.

Special attention has to be drawn to unwanted transient 'objects' like cosmics. Often they can be filterd out using the known characteristics of brightness and of sharpness.

3.2. Results from simulations

In order to assess the detection limit in a quantitative way a series of simulations was performed: Images were generated using parameters derived from actual observations. The characteristics of these 'frames' do in fact not differ from real observations. In this and the following sections the detection limit will be expressed in terms of the signal-to-noise ratio where the latter is defined separately for the two different search methods as explained in section 3.1. (not to be confused with the signal-to-noise ratio associated with an individual pixel!). The calculations are based on a telescope of 1m diameter and of 4m focal length. The pixel size has been taken as 20 x 20μm giving a scale in the focal plane of about 1 arcsec/pixel. The width of an object (FWHM) was set to 2 arcsec, thus covering two pixels.

The following values were adopted for the simulation:

- readout noise of the CCD camera: 5 electrons $sec^{-1}pixel^{-1}$
- sky background: 2000 photons $sec^{-1}m^{-2}arcsec^{-2}$ in the spectral band covered by the camera.

The latter value corresponds to a sky that is about seven times brighter than the dark night sky, a reasonable value for the nautical twilight (sun about 15° below the horizon).

The transformation of visual magnitudes to irradiance was defined using a source with a solar spectrum and the spectral quantum efficiency of our CCD camera together with a combined transmission coefficient of the atmosphere and the telescope of 50%. With these assumptions a visual magnitude of 10^m corresponds to an irradiance of 10^{-6} photons $sec^{-1}m^{-2}$ or $3.9 \cdot 10^{-15}$ W $m^{-2}nm^{-1}$ in the V-band.

For the connection between the visual magnitude m and the dimension d of an object an albedo of 0.3 has been adopted from (Ref. 1). Considering the potentially large range for the albedo for different materials and surface properties, this dimension d could significantly deviate from our adopted value. The diameter of an object at a given distance and a given irradiance is proportional to the inverse square root of the albedo.

The signal-to-noise ratio for an object with a given brightness is determined by the exposure time for a given instrument, camera and sky brightness. One possibility to improve the signal to noise ratio and hence the detectability of an object is to increase the integration time. There are two limitations doing this however: the sky background which may saturate the detector and the angular velocity of the object with respect to the trajectory of the telescope.

To detect fainter objects in a geosynchronous orbit the exposure time can easily be increased because of the slow angular velocity of those objects with respect to a fixed telescope. An object of the same size in a lower orbit is brighter but the higher angular velocity cancel most of this advantage, unless the telescope is tracking the object. But perfect tracking when looking for objects with unknown trajectories is obviously not possible; a tracking with the expected mean velocity for a given population of objects (space debris) might be feasible.

m_V	d	(a) 1.7 rms		(b) 3x3 filter	
	[cm]	1sec	5sec	1sec	5sec
12	120	230.	515.	245.	547.
13	75	112.	251.	123.	275.
14	50	58.	129.	56.	125.
15	30	25.	55.	24.	53.
16	20	11.	23.	9.7	22.
17	12	4.5	10.	3.9	8.8
18	8	.	4.1	1.6	3.5
19	5	.	.	.6	1.4
20	3	.	.	.3	.6

Table 1. Signal to noise ratios for objects in geostationary orbit for two different algorithms and two exposure times using a 1m telescope.

Signal-to-noise ratios for objects in the geostationary ring are given in Table 1. The results refer to exposure times 1 sec and 5 sec and for the two search algorithms discussed above: (a) scanning of the image for pixel intensities exceeding the mean background by 1.7 times the rms of the background and collecting all adjacent ones belonging to the same object. (b) scanning the image with a 3x3 filter. We assumed that the objects stay in the same pixel during exposure, i.e. that it does not

move with more than 1 arcsec/sec and .2 arcsec/sec for the exposure times 1 sec and 5 sec respectively.

In the case (a), the signal-to-noise ratio of a detectable object may be as low as 2.5 to 4, depending on the object position relative to the pixel boundaries. Objects with lower values escape detection because all pixels lie below the threshold (indicated by dots in the table).

In case (b) the signal to noise ratio is larger compared to case (a) for bright objects and smaller for the weak ones. This is a consequence of the different definitions of the signal-to-noise ratios: the values of the first method correspond to the actual object whereas the second method yields values with respect to the 9 pixel sized filter mask. In the filter method the additional noise from 'object free' pixels play a dominant role at the faint end. Using a 3x3 filter we may nevertheless detect much fainter objects than with method (a) because even a pixel with signal-to-noise ratio of .8 still belongs to an object (with a significance of 99%). We may thus conclude from Table 1, that the detection of objects as small as 5cm in a strictly geostationary orbit is still possible (5 seconds of integration). One should not neglect however the big effort necessary in the image processing part. Furthermore, highest accuracy is needed in the determination of the mean background intensity and its rms. This task may not be trivial at all, considering that unresolved (diffuse!) background sources may be present or that detector gain may be pixel dependent and variable with time.

Table 2 contains the signal-to-noise ratios calculated for an object in a 500 km orbit moving at 2900 arcsec/sec with respect to the telescopes pointing direction. Results are given for the same two algorithms as in Table 1 and for exposure times of 0.01 and 0.05 seconds.

m_V	d	(a) 1.7 rms		(b) 3x3 filter	
	[cm]	.01sec	.05sec	.01sec	.05sec
5	42.	873.	1911.	262.	264.
6	26.	542.	1144.	164.	162.
7	17.	330.	647.	101.	95.
8	11.	198.	365.	61.	52.
9	6.6	111.	177.	34.	26.
10	4.2	56.	84.	18.	12.
11	2.6	27.	36.	8.3	4.9
12	1.7	.	.	3.6	2.0
13	1.1	.	.	1.5	.8
14	0.7	.	.	.6	.3

Table 2. Signal to noise ratios for objects in a 500 km orbit moving with 2900 arcsec/sec for two different algorithms and two exposure times using a 1m telescope.

Because of the object's rapid motion the exposure times must be very short and should at optimum be limited to the time the object stays in one pixel. Additional integration time only adds noise from the sky background. For fast moving objects, on-chip binning increases the signal by the binning factor but the noise from the sky background is increased by the same factor and thus the only improvement stems from the reduction of the readout noise. The readout noise plays no significant role for integration times greater than 0.05 sec.

In case (a) it is at first glance surprising that the limiting signal-to-noise ratio is quite high. This may be explained by the very large extent of the (trailing) object which results in a small intensity share for each individual pixel that therefore fail to reach the threshold. With the filter technique only a small part of the entire trail is sampled (the trail is about 30 or 150 pixels respectively long!) but nevertheless objects with a size down to 1cm may be observed. We should mention that the same reservations concerning the background are valid as for the GEO orbits.

4. INSTRUMENTATION

There is an ongoing project at the Astronomical Institute of the University of Berne called 'optical astrometry of fast moving objects'. Although it focuses primarily on precise position determination of 'known' objects, the techniques under development potentially are very well suited for space debris tracking too.

For test observations we use the Satellite Laser Ranging Telescope of the Zimmerwald observatory near Berne which is in routine operation, contributing data to the NASA Crustal Dynamics Project and other geodynamic projects. The instrument is a Cassegrain type telescope with a primary mirror of 0.525 m diameter and 1.0 m focal length. The alt-azimut mount with DC servo disc motors allows a maximal slewing rate of 8 deg/sec. The encoders have a resolution of 0.001 deg.

Image acquisition is performed with a CCD camera, using a PHOTOMETRICS PM512 front side illuminated CCD detector. Its dimensions are 512 x 512 pixels with a pixel size of 20 x 20 μm. The camera is cooled to -45° C with a thermoelectric element and a secondary liquid cooling circulation. With the current telescope the mapping scale is 4.1 arcsec/pixel and the field of view is 35' x 35'.

The entire system consists, apart from telescope and camera, of a camera control computer (68040 VME bus system) for image acquisition, processing and management, a CAMAC interface system containing event timers for the epoch registration and a station computer (microVAX). The latter is used for the real time telescope and camera control tasks like positioning and object tracking as well as for off-line ephemerides calculations, for the selection of reference stars for astrometric measurements, and for data reduction. Precise epoch registration is guaranteed by the station clock subsystem used for satellite laser ranging (better than 1 microsec within UTC).

A considerable amount of time was spent for software developments. In particular spezialized modules for data acquisition, image processing, object recognition, centroid determination and for data reduction were needed. We have to deal with a special problem: the short exposure times lead to high data rates (up to several frames per second). Storing all this data would be unpossible especially when considering that we are in fact interested in an extremely small fraction of the recorded information only. When searching for unknown objects only distinct signatures in the difference of two (nearly identical!) frames are of importance. Moreover the final result of an observation consists of a few numbers characterizing the object, its position and possibly its angular velocity. These facts, together with the required follow-up observations for newly discovered objects (whithin seconds after their discovery!) clearly ask for a real time processing approach. The software system was therefore designed as a set of individual modules, each resposible for one of

the above mentioned tasks. These modules are running concurrenly in a real time environment on the camera control computer. This solution not only provides results shortly after the observation but also allows to close the loop and control the telescope, the image acquisition, etc. according to information from already processed frames (the latter is essential for quick follow-up observations). Extensive off-line data reduction facilities are available for more detailed studies.

5. OBSERVATIONS OF SATELLITES

We started to observe satellites in known orbits to test the developed techniques. Most of our observations are concentrated near the geostationary ring, i.e. of objects in GEO orbits and at apogee of GTO orbits. The reason to restrict the study to these orbits is twofold: (a) the objects have lower angular velocities than in LEO, (b) LEO objects may be observed during dusk and dawn only, and in order to cover the whole inclination range, an observation site must be close to the equator.

A few observations of lower orbiting satellites such as LAGEOS (see Figure 1.) were made. The CCD image shows the satellite and the stars passing close to it. The 13.5 magnitude satellite was tracked at about 170 arcsec/sec during the 0.5 second exposure. Thus the object of interest appears pointlike whereas the stars are elongated.

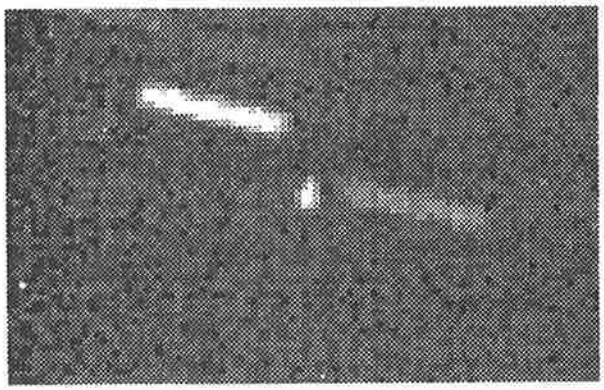

Figure 1. 0.5 second exposure of LAGEOS and of several star trails at the 0.5m Laser ranging telescope in Zimmerwald. The image represents approximately a 7' x 4' area. Pixel size is 4.1".

Figure 2 shows the two geostationary telecomunication satellites Tdf-1 and Tdf-2 as points in front of the moving background of stars. The telescope was fixed during this 5 second exposure. The distance between the two satellites is only about 1 arcmin corresponding to 10 km projected to the geostationary belt. Astrometric observations of co-located satellites could provide high precision relative orbit information and support collision prevention efforts, thus helping to eliminate potential sources of future space debris.

In Figure 3 the results of the astrometric position determinations of the inoperative satellite Intelsat 4a f-6 are shown. The object has a size of 2.8m x 2.4m, it is in an uncontroled orbit in the geostationary ring. The series of ten observations spans 50 seconds. During this time interval the satellite moved about 16 arcsec in southward direction in its orbit which is inclined to the equatorial plane by about 6°. The individual frames were exposed for 1.5 sec which give rise to a signal-to-noise ratio for the satellite of about 32.

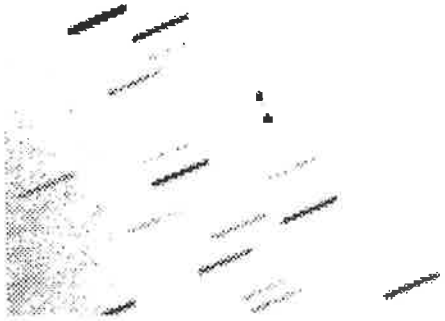

Figure 2. The two geostationary telecommunication satellites Tdf-1 and Tdf-2, seen in this negative print as points in front of the moving background of stars. The telescope was fixed during this 10 second exposure. The distance between the two satellites is about 1 arcmin only. The image covers approximately an area of 20' x 13'.

Figure 4 contains the positions of all geostationary objects observed with our telescope during three nights in February and March 1993. 43 objects were 'detected'. The majority of them could be identified using the "Log of Objects near the Geostationary Ring" from ESOC (Ref. 2) which is based on the NASA two line elements. Large structures as the Eutelsat satellites are easily detectable. Several faint and slow moving objects were detected too, but they could not yet be identified.

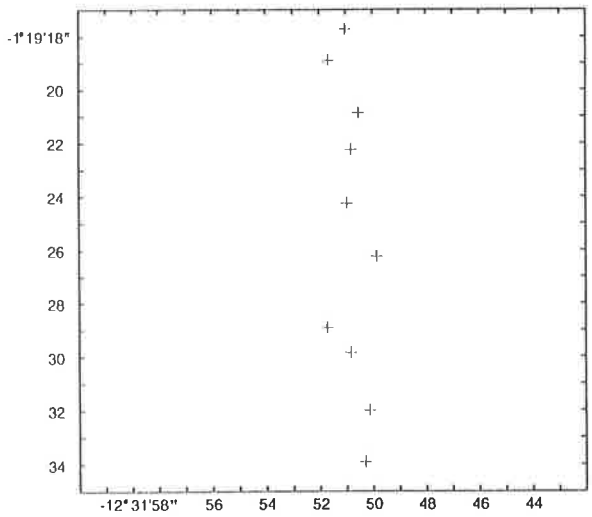

Figure 3. Astrometric position of the geostationary satellite Intelsat 4a f-6. The time span of the ten observations is about 50 sec. Hour angle is in x-direction and declination in y-direction. Tick marks are in arcseconds. The error bars of about ± 0.3" indicate the statistical error of a single observation.

Objects in GTO orbit may be detected from midlatitudes most easily when they are in the apogee. There they reach their maximum elevation whereas their motion is a minimum. A satellite in a GTO orbit moves at his apogee with about 7 arcsec/sec with respect to a fixed telescope, i.e. with about half of the siderial rate. Such objects may thus be spotted with a fixed telescope much like a GEO object.

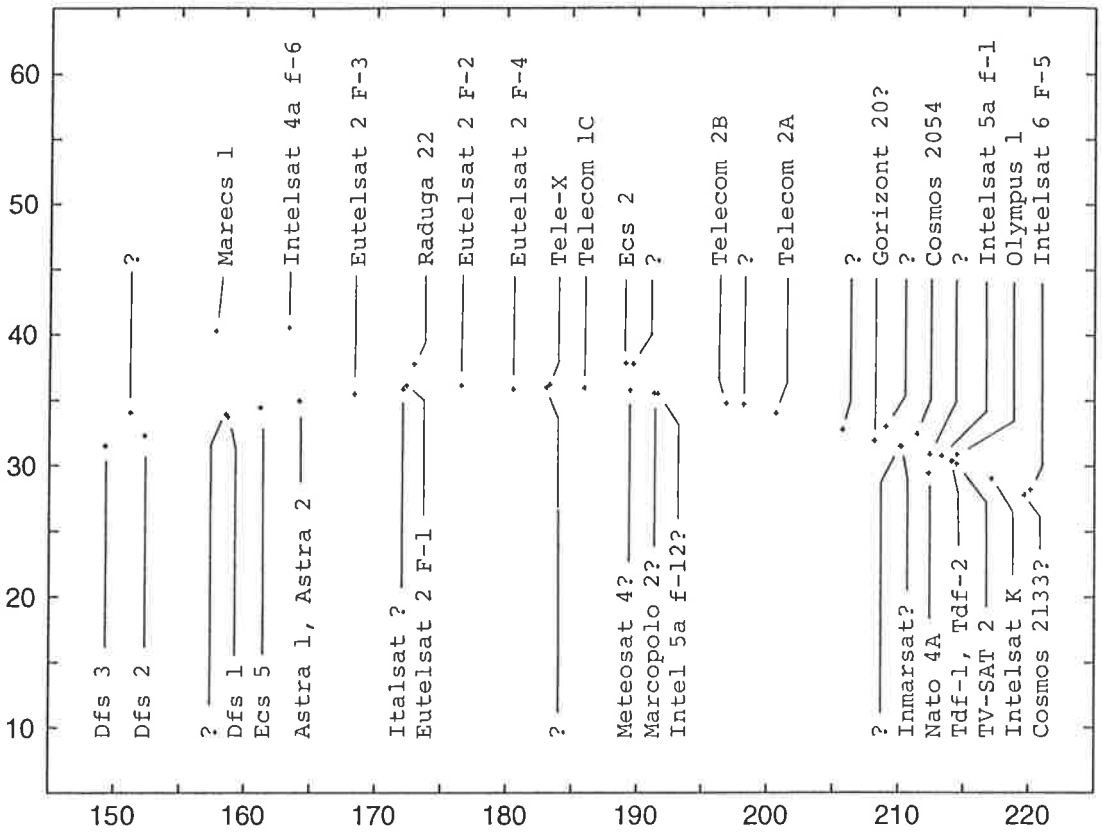

Figure 4. Geostationary satellites observed with the Laser ranging telescope in Zimmerwald during three nights. Azimut is in x-direction, elevation in y-direction. Identifications are based on the "Log of Objects near the Geostationary Ring" from ESOC.

6. CONCLUSIONS

The simulations show that it is feasible to observe objects down to a size of 5 cm in GEO or GTO and down to 1 cm in LEO (assuming an albedo of 0.3) using a moderate size telescope of 1 m aperture and CCD image procesing techniques. The necessary effort for telescope control, data acquisition and real time processing, specially when observing objects in LEO, is considerable. Measurements stemming from the experimental setup at the Zimmerwald Laser telescope clearly demonstrate the potential of the technique.

7. REFERENCES

1. Lobb, D.R. (Ed.), Study on Optical Sensors for Space Debris Observation, Sira Ldt., Nov. 1992.

2. Log of Objects near the Geostationary Ring, ESOC, Dec. 1992.

3. Verdun, A, Objekterkennung und Zentroidbestimmung bei CCD-Richtungsbeobachtungen, Lizentiatsarbeit, AIUB, Feb. 1993.